JACC: BASIC TO TRANSLATIONAL SCIENCE VOL. 5, NO. 5, 2020

PRECLINICAL RESEARCH

Activation of Oxytocin Neurons Improves Cardiac Function in a Pressure-Overload Model of Heart Failure

Jhansi Dyavanapalli, PHD,[a] Jeannette Rodriguez, BS,[b,*] Carla Rocha dos Santos, PHD,[a,*] Joan B. Escobar, MSC,[a] Mary Kate Dwyer, BS,[b] John Schloen, BS,[b] Kyung-min Lee, MD,[a] Whitney Wolaver, BS,[a] Xin Wang, MD,[a] Olga Dergacheva, PHD,[a] Lisete C. Michelini, PHD,[c] Kathryn J. Schunke, PHD,[b] Christopher F. Spurney, MD,[d] Matthew W. Kay, DSC,[b] David Mendelowitz, PHD[a]

VISUAL ABSTRACT

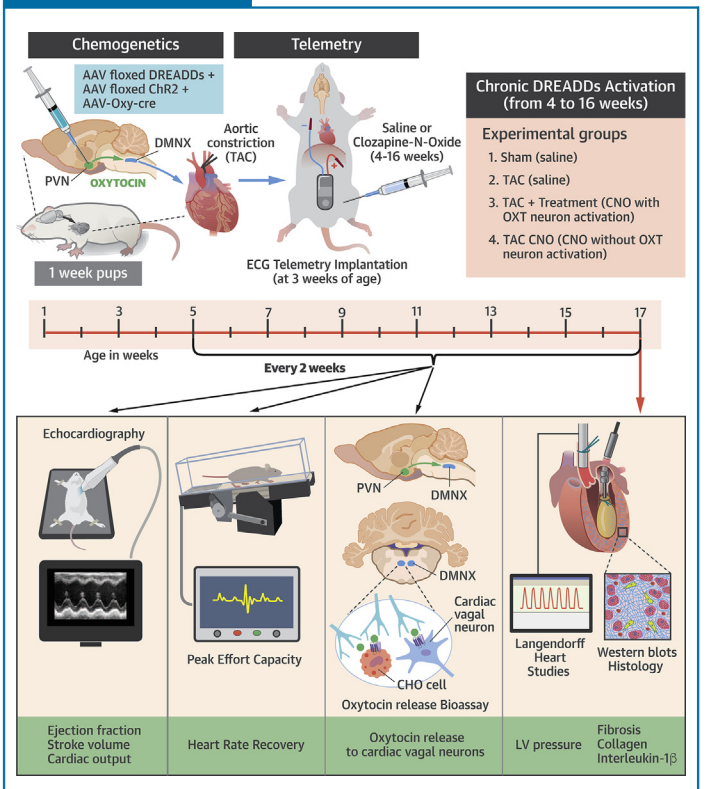

Dyavanapalli, J. et al. J Am Coll Cardiol Basic Trans Science. 2020;5(5):484–97.

HIGHLIGHTS

- **Hypothalamic OXT neurons were chronically activated using a chemogenetic approach in an animal model of HF.**
- **Synaptic release of OXT onto parasympathetic autonomic targets was reduced in animals with HF but restored with daily treatment consisting of activation of OXT neurons.**
- **Long-term daily OXT neuron activation increased parasympathetic activity to the heart and reduced mortality, cardiac inflammation, and fibrosis and improved critical longitudinal *in vivo* indices of cardiac function.**
- **The benefits in cardiac function and autonomic balance in HF closely tracked the study-designed differences in initiation of OXT neuron activation in different groups.**

ISSN 2452-302X https://doi.org/10.1016/j.jacbts.2020.03.007

SUMMARY

This work shows long-term restoration of the hypothalamic oxytocin (OXT) network preserves OXT release, reduces mortality, cardiac inflammation, fibrosis, and improves autonomic tone and cardiac function in a model of heart failure. Intranasal administration of OXT in patients mimics the short-term changes seen in animals by increasing parasympathetic—and decreasing sympathetic—cardiac activity. This work provides the essential translational foundation to determine if approaches that mimic paraventricular nucleus (PVN) OXT neuron activation, such as safe, noninvasive, and well-tolerated intranasal administration of OXT, can be beneficial in patients with heart failure. (J Am Coll Cardiol Basic Trans Science 2020;5:484–97)

ABBREVIATIONS AND ACRONYMS

ANOVA = analysis of variance
CHO = Chinese hamster ovary
ChR2 = channelrhodopsin
CNO = clozapine-N-oxide
CVN = cardiac vagal neuron
DMNX = dorsal motor nucleus of the vagus
DREADD = designer receptors exclusively activated by designer drug
HF = heart failure
IL = interleukin
LV = left ventricle
LVDP = left ventricle-developed pressure
PVN = paraventricular nucleus of the hypothalamus
OXT = oxytocin
SD = standard deviation
TAC = transascending aortic constriction

The 9-amino acid neuropeptide, oxytocin (OXT), is only synthesized in a limited number of discrete brain regions: the paraventricular (PVN), supraoptic, and accessory nuclei of the hypothalamus (1). In addition to the classic effects of OXT—such as uterine contraction, milk ejection during lactation, sexual arousal, and penile erection—recent work indicates that OXT has an important role in both behavior and cardiovascular homeostasis, particularly during anxiety and stress (2). In human volunteers in unstressed conditions, intranasal administration of OXT increased parasympathetic—and decreased sympathetic—cardiac control (3). Administration of OXT to subjects with obstructive sleep apnea shortened the duration of obstructive events and increased sleep satisfaction and parasympathetic activity to the heart (4).

The potential benefit of long-term OXT network activation in protracted cardiovascular diseases has not been tested. Heart failure (HF) affects nearly 23 million people worldwide, and prevalence is projected to increase 46% in the next 15 years (5). Approximately 50% of patients diagnosed with HF die within 5 years, necessitating the development of new treatments (5). A hallmark of HF is elevated cardiac sympathetic activity and parasympathetic withdrawal (6,7), an imbalance that contributes to ventricular dysfunction, structural remodeling, and electrical instability (8). In the initial stages of HF, parasympathetic tone decreases as early as 3 days after the development of cardiac dysfunction, typically preceding increases in sympathetic activity (9,10).

Here, using OXT-sensitive sniffer cells, we test the hypothesis that endogenous release of OXT from hypothalamic PVN neurons onto brainstem autonomic targets is blunted in an animal model of HF. Furthermore, we examine if chronic chemogenetic activation of PVN OXT neurons restores OXT release and if novel treatment paradigms of restoring OXT neuron activity, initiated at different intervals during the disease-progression timeline, reduces mortality, cardiac inflammation and fibrosis, and longitudinal indices of cardiac dysfunction compared with untreated animals with HF.

From the [a]Department of Pharmacology and Physiology, George Washington University, Washington, DC; [b]Department of Biomedical Engineering, George Washington University, Washington, DC; [c]Department of Physiology, Biophysics, Institute of Biomedical Sciences, University of Sao Paulo, Sao Paulo/SP, Brazil; and the [d]Children's National Heart Institute, Center for Genetic Medicine Research, Children's National Health System, Washington, DC. *Ms. Rodriguez and Dr. Rocha dos Santos contributed equally to this work and are joint second authors. This work was supported by an American Autonomic Society postdoctoral fellowship (to Dr. Dyavanapalli), a predoctoral fellowship from the Coordenação de Aperfeiçoamento de Pessoal de Nível Superior-Brasil (CAPES) (to Dr. Rocha dos Santos), AHA SDG 18CDA34080353 (to Dr. Schunke), and NIH R01HL133862 (to Drs. Mendelowitz and Kay). The authors have reported that they have no relationships relevant to the contents of this paper to disclose.
The authors attest they are in compliance with human studies committees and animal welfare regulations of the authors' institutions and Food and Drug Administration guidelines, including patient consent where appropriate. For more information, visit the *JACC: Basic to Translational Science* author instructions page.

Manuscript received January 14, 2020; revised manuscript received March 6, 2020, accepted March 6, 2020.

JACC: BASIC TO TRANSLATIONAL SCIENCE VOL. 5, NO. 5, 2020
MAY 2020:484–97

METHODS

ETHICAL APPROVAL. All animal procedures were completed in agreement with the George Washington University institutional guidelines and in compliance with the panel of Euthanasia of the American Veterinary Medical Association and the National Institutes of Health (NIH) Guide for the Care and Use of Laboratory Animals.

SURGICAL PROCEDURE FOR TRANSASCENDING AORTIC CONSTRICTION. Pressure overload induced left-ventricular (LV) hypertrophy was initiated in male Sprague-Dawley rats using a minimally invasive transascending aortic constriction (TAC) procedure, similar to our previous study (11). Rats at 1 week of age were anesthetized by hypothermia and underwent TAC surgery. A 0.5-cm incision was made at the level of the chest, the chest was opened, and the thymus was retracted to reveal the aorta. A 4-0 silk suture was passed around the ascending aorta, and—with a 25-gauge needle temporarily placed adjacent to the aorta—the suture was tied around both the aorta and needle (TAC and TAC + OXT groups). The needle was then removed, leaving the constricting suture around the aorta. Buprenorphine was applied as an analgesic. Successful constriction was confirmed with high aortic-velocity post constriction, using high-resolution echocardiography as well as upon examination of the aorta after each animal was killed.

SELECTIVE EXPRESSION AND ACTIVATION OF ChR2 AND DREADDs IN PVN OXT NEURONS. Selective expression of both channelrhodopsin (ChR2) and an excitatory chemogenetic receptor for chronically activating PVN OXT neurons, designer receptors exclusively activated by designer drugs (DREADDs), was accomplished using 3 viral vectors in combination with the Cre-Lox system (NIH, Bethesda, MD). Expression of the enzyme Cre recombinase was exclusively driven by the OXT promoter (rAAV1-OXT-Cre), stereotactically coinjected into the PVN of 1-week old pups with both floxed excitatory ChR2 (AAV1-EF1a-DIO-hChR2) and floxed excitatory DREADDs (AAV2-hSyn-DIO-hM3D(Gq), (30 to 50 nl of each virus selectively microinjected over a 20-min period), as previously described (12).

ACTIVATION OF PVN OXT NEURONS IN VIVO. PVN OXT neurons expressing DREADDs were exclusively activated by clozapine-N-oxide (CNO), 1 mg/kg intraperitoneally (IP). Our previous work has demonstrated that injections of CNO increases the firing of PVN OXT neurons for at least 1 h (12).

IN VIVO ASSESSMENTS OF CHANGES IN AUTONOMIC TONE AND CARDIAC FUNCTION. Sprague-Dawley rats at 2 weeks post-TAC/Sham surgery were anesthetized (isoflurane) and implanted with a telemetry device (DSI wireless transmitters, ETA-F10 [Data Sciences International, St. Paul, Minnesota]) with electrocardiographic (ECG) leads inserted subcutaneously to measure heart rate (HR). The following protocol was used to measure peak effort capacity, defined as the time that animals are able to run on the treadmill and the speed at time of exhaustion. Animals began with an initial warm-up period of 5 min at 6 cm/s with 1 min of recuperation. The treadmill speed then quickly ramped up to 12 cm/s and increased by 6 cm/s every 3 min until exhaustion. Heart rate recovery (HRR) was assessed by subtracting the instantaneous HR following 20 s of recovery from that at peak exercise (Naughton protocol).

Echocardiographic measurements were obtained using a VisualSonics high-resolution small-animal system (Vevo 3100 Imaging System, FUJIFILM Visual Sonics Inc, Toronto, Ontario, Canada) that continuously acquired the ECG, respiratory waveform, and body temperature. Imaging was performed at frame rates up to 1KHz, using 25MHz linear array transducer to obtain 2-dimensional (2D) pulse and continuous-wave Doppler and Motion-mode (M-mode) imaging. A 2D parasternal long-axis view of the LV was used to obtain LV outflow tract diameter and cardiac functional measures including percent LV ejection fraction (EF %). M-mode images were obtained from the parasternal short-axis view of the LV, at the level of papillary muscles to measure LV structural variables including LV diastolic posterior-wall diameter (LVPWd), interventricular septal diameter (IVSd), LV diameter in diastole (LVDd) and systole (LVDs), and LV systolic posterior-wall (LVPWs) thickness. These parameters were used to calculate percent of fractional shortening (FS). Pulse-wave Doppler imaging in an apical 4-chamber view was used to obtain inflow velocities through mitral valves for assessing diastolic function, including early diastolic mitral inflow (E-wave), late diastolic mitral inflow (A-wave), and early-to-late diastolic mitral inflow ratio (E/A ratio). Continuous-wave Doppler modality was used to measure functional variables, such as velocity and pressure of blood flow in the ascending and descending aorta, and HR and cardiac output.

EX VIVO ASSESSMENTS OF CARDIAC FUNCTION. At 16 weeks post-Sham/TAC, rats were anesthetized with an IP injection of pentobarbital (50 mg/kg) and isoflurane inhalation anesthesia. Following cessation of pain reflexes, hearts were rapidly excised and Langendorff perfused via the aorta at constant pressure (65 mm Hg) and temperature (37°C [98.6°F]) with a

FIGURE 1 Chemogenetic Hypothalamic Oxytocin Neuron Activation Restores Oxytocin Release to Cardiac Vagal Neurons in Heart Failure

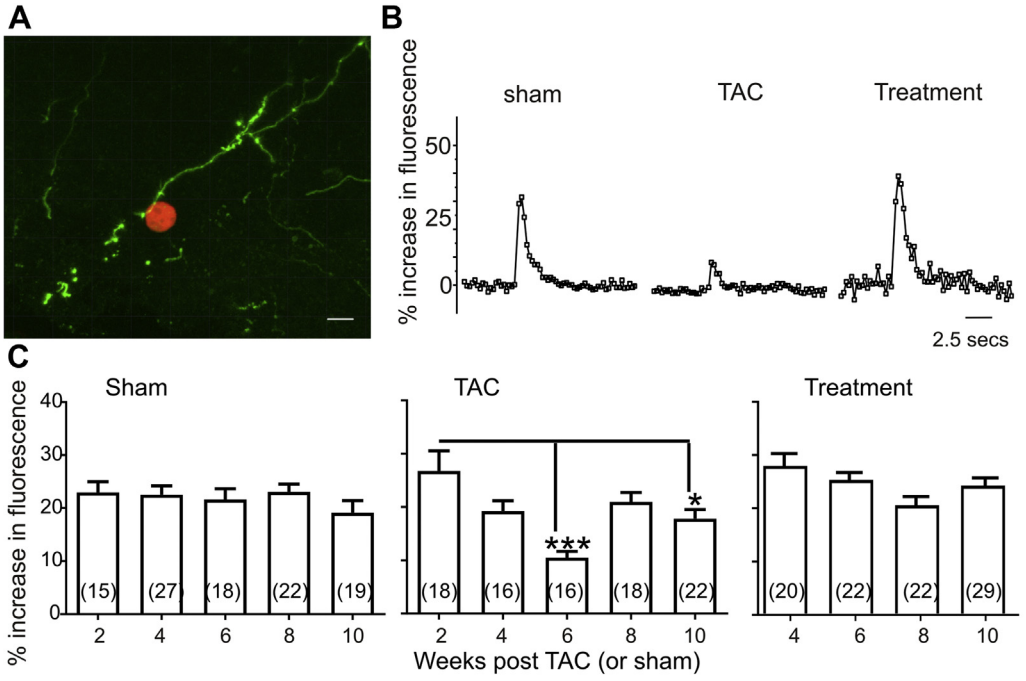

(A) Three-dimensional (3D) confocal image showing sniffer CHO cell **(red)** expressing R-GECO and oxytocin receptor in close proximity to channelrhodopsin expressing PVN oxytocinergic nerve fibers **(green)** projecting to brainstem DMNX cardiac vagal neurons. Scale bar represents 10 microns. **(B)** Optogenetic stimulation of ChR2 expressing PVN oxytocin fibers projecting to cardiac vagal neurons evokes an increase in intracellular calcium response in sniffer CHO cells that were significantly blunted in animals with HF at 6 weeks post-TAC. These responses were restored in the treatment group upon chemogenetic activation of DREADDs-expressing PVN oxytocin neurons starting at 4 weeks post-TAC. DREADDS was activated by daily intraperitoneal injections of CNO (1 mg/kg) to treatment animals, whereas Sham and TAC animals received saline injections. Responses representative of 1 sniffer CHO cell are shown. **(C)** Quantitative histograms showing increase in fluorescence in CHO cells evoked by photostimulation of PVN oxytocin fibers at various time points of disease progression (2, 4, 6, 8, and 10 weeks post-TAC/Sham) in Sham, TAC, and 4 to 10 weeks post-TAC in treatment-group animals. Responses in Sham animals were not different in all time points. TAC animals displayed blunted responses at 6 and 10 weeks post-TAC compared with 2 weeks post-TAC. Similar to Sham animals, responses were not different in treatment animals at all time points. Data were analyzed using mixed-effects model with Tukey's postmultiple comparison test. Numbers in parentheses indicate number of cells. Number of animals in each group of animals at each time point are Sham ($n = 3$ at all points except 6 weeks [n=4]); TAC ($n = 3$ except at 8 weeks [$n = 4$]); treatment ($n = 3$ at all time points); *$p < 0.05$; ***$p < 0.001$. CHO, Chinese hamster ovary; DREADDs, designer receptors exclusively activated by designer drugs; HF, heart failure; PVN, paraventricular nucleus of the hypothalamus; R-GECO, red fluorescent genetically encoded Ca2+ indicators; TAC, transascending aortic constriction.

Krebs-Henseleit solution containing (in mM) 118 NaCl, 4.7 KCl, 1.25 $CaCl_2$, 0.57 $MgSO_4$, 1.17 KH_2PO_4, 25 $NaHCO_3$, and 6.0 glucose. Perfusate was oxygenated with 95% O_2-5% CO_2. After a stabilization period of 10 min, a size-5 balloon (Harvard Apparatus, Holliston, MA) was inserted into the LV to measure isovolumic LV-developed pressure (LVDP), as we have previously described (13,14). Diastolic pressure was set to 7 mm Hg, and LVDP was computed as the difference between systolic and diastolic pressures. HR and LVDP were measured for at least 15 min during sinus rhythm. After each study, contractility and relaxation were calculated as the maximum and minimum values of the first derivative of the LVDP waveform, respectively, to assess inotropy and lusitropy.

ANATOMIC MEASUREMENTS AND HISTOLOGY. Hearts from ex vivo studies were sliced longitudinally, halfway between the anterior and posterior sides. One-half of the heart was preserved in 10% formalin and stained with Masson's trichrome to visualize collagen deposition.

WESTERN BLOTTING. Hearts from ex vivo studies were sliced longitudinally, halfway between the anterior and posterior sides. LV tissue from one-half

FIGURE 2 Long-Term Chemogenetic Activation of PVN Oxytocin Neurons Attenuates Cardiac Dysfunction Seen in Animals With Heart Failure

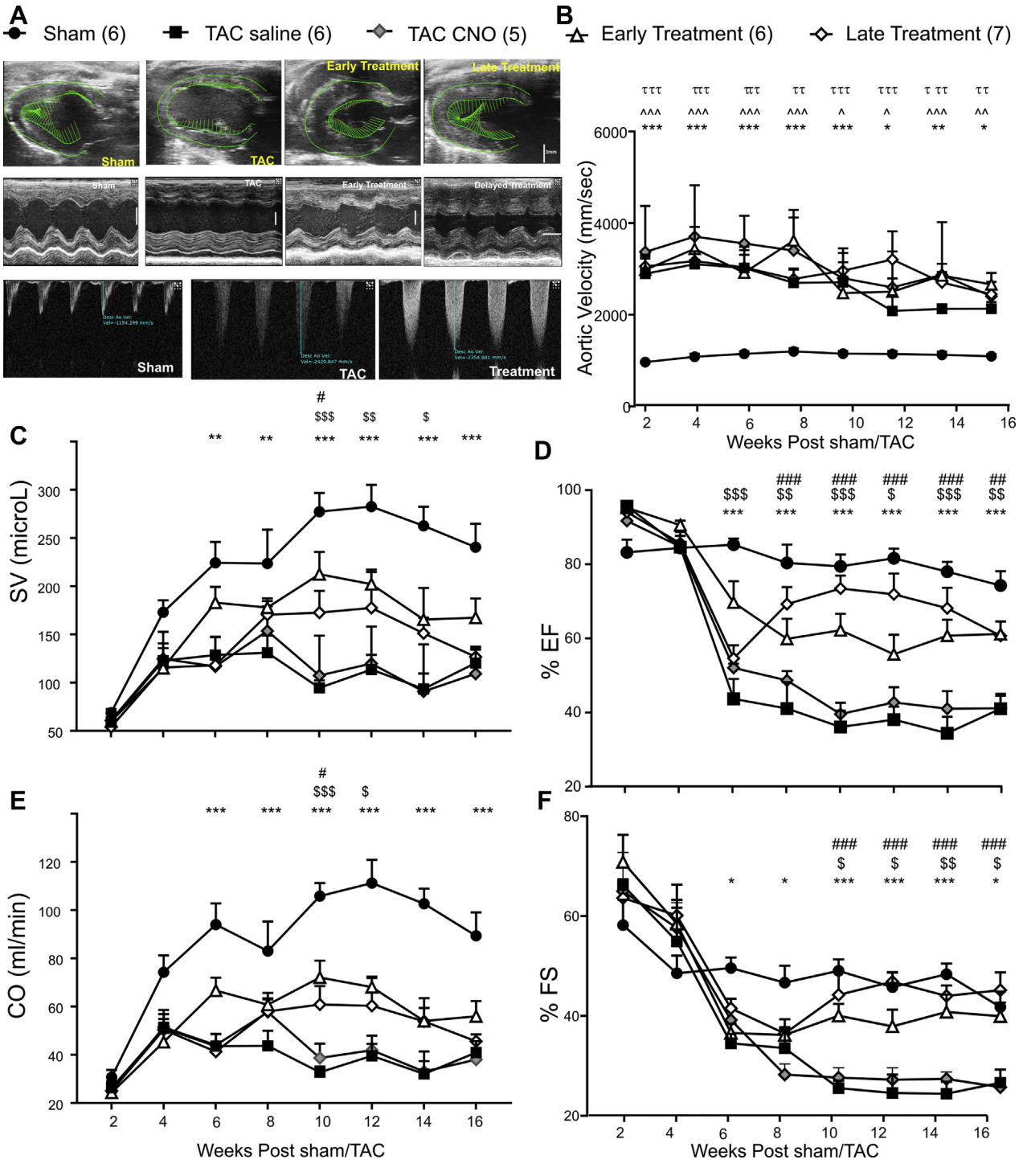

Continued on the next page

of the heart were flash frozen in liquid nitrogen and stored at -80°C (-112°F). Samples were thawed and homogenized using the Qproteome Mammalian Protein Prep Kit (QIAGEN, Hilden, Germany) in tubes containing metallic beads. Samples were centrifuged at 14,000 g for 10 min, and protein concentrations were determined by the Pierce BCA Protein Assay (Thermo Fisher Scientific, Waltham, Massachusetts). Laemmli buffer (Bio-Rad, Hercules, California) with 10% 2-mercaptoethanol (Sigma-Aldrich, St. Louis, Missouri) was added to the samples, which were then heated to 98°C (208.4°F). Equal protein concentration was loaded into wells containing 4% to 15% PROTEAN or Criterion TGX Gels (Bio-Rad). The samples were then run between 50V to 100V for up to 2 h to separate proteins by electrophoresis.

After electrophoresis, the samples were then transferred to polyvinylidene fluoride (PVDF) membranes, using the Trans-Blot Turbo Transfer System (Bio-Rad). The membranes to be probed for collagen III (Abcam, Cambridge, United Kingdom) were blocked with 5% milk for 18 h and then incubated for 1 h at room temperature with collagen III, at a concentration of 1:1,000. The membranes to be probed for interleukin(IL)-1β were blocked with 5% bovine serum albumin (BSA) for 2 h. They were then incubated with IL-1β (Cell Signaling Technology, Danvers, Massachusetts) at a concentration of 1:1,000 overnight at 4°C (39.2 °F). All membranes were washed and incubated for 1 h with the horseradish peroxidase (HRP)-conjugated secondary antibodies anti-rabbit 1:6,000 and anti-mouse 1:6,000 (Santa Cruz Biotechnology, Dallas, Texas). The membranes were washed again, and gels were imaged using an Azure cSeries c600 (VWR, Radnor, Pennsylvania) gel imager. The membranes were stripped with a mild stripping buffer containing 0.2 M glycine (Sigma-Aldrich), 3.5 mM sodium dodecyl sulfate (Bio-Rad), and 1% Tween 20 (Sigma-Aldrich). They were then reblocked with 5% milk for 19 h and incubated with glyceraldehyde-3-phosphate dehydrogenase (GAPDH) antibody (Sigma-Aldrich) 1:6,000 for 1 h. The membranes were washed and incubated for 1 h with the anti-rabbit HRP-conjugated secondary antibody. Band intensities for collagen III and IL-1β were measured using NIH ImageJ or Li-Cor Image Studio (LI-COR Biosciences, Lincoln, Nebraska) and normalized to the corresponding band intensity for GAPDH; collagen III bands were normalized to Sham values as well as GAPDH.

Because of the large number of animals in each group, not all samples could be loaded on the same gel. We therefore ran 2 to 3 gels and included samples from each of the 3 groups (Sham, TAC, and TAC + OXT) on each gel and repeated selected samples on each gel. We then normalized signal intensity between membranes based on the repeated sample expression. This method provides consistent normalization of all samples both within each set and across the minimum number of required gels. Refer to Supplemental Figure 1 for more details.

STATISTICAL METHODS. Data were presented as mean ± standard error mean and analyzed using GraphPad Prism (GraphPad, San Diego, California) statistical software (version 8). Longitudinal data were compared among all groups using mixed-effects model (restricted maximum likelihood method) with Tukey's postmultiple comparison test. For survival analysis, Kaplan-Meier curves were plotted and compared, using the log-rank test. One-way analysis of variance (ANOVA) was used to compare in vitro heart data statistically from Langendorff and Western-blot studies. A p value of ≤0.05 was considered statistically significant.

FIGURE 2 Continued

(A) The **top panel** depicts high-resolution 2D echocardiograms in parasternal longitudinal-axis B mode taken from 16-week post-Sham, TAC, early activation of DREADDs-expressing PVN oxytocin neurons (initiated at 4 weeks post-TAC), and late treatment (starting at 6 weeks post-TAC) animals showing left ventricle (LV) in mid-systole with directional vectors in green. Vertical scale bar represents 3 mm. The **middle panel** shows 2D echocardiograms in parasternal short-axis M-mode at 16 weeks post-Sham, TAC, early- and late-treatment animals, used to measure the LV posterior-wall thickness and interventricular septal-wall thickness, LV internal diameter, and percent fractional shortening. Vertical and horizontal scale bar represents 3 mm and 0.1 sec, respectively. The **bottom panel** displays pulsed Doppler measurements of descending aortic flow velocities taken immediately after TAC point in Sham, TAC, and treatment animals. **(B)** Quantitative longitudinal Doppler descending aortic flow velocities in Sham, TAC saline (expressing DREADDs), TAC CNO (not expressing DREADDs), early- and late-treatment animals taken biweekly from 2 to 16 weeks post-Sham/TAC surgery. The velocities were 3-fold greater in TAC and treatment animals compared with Sham animals. Graphs displaying longitudinal echocardiographic measurements of stroke volume **(C)**, percent ejection fraction **(D)**, cardiac output (CO) **(E)** from parasternal longitudinal axis B-mode and percent fractional shortening from parasternal short-axis M-mode measured biweekly from 2 to 16 weeks post-Sham, TAC saline (expressing DREADDs), TAC CNO (not expressing DREADDs), and early- and late- treatment animals. Data were analyzed using mixed-effects model with Tukey's multiple comparison post-test. Sham (n = 6); TAC (n = 6); early treatment (n = 6); late treatment (n = 7); TAC CNO (n = 5);. *Sham vs. TAC; $TAC vs. early treatment; #TAC vs. late treatment; ^Sham vs. early treatment; τSham vs. late treatment; *p < 0.05; **p < 0.01; ***p < 0.001. CNO, clozapine-N-oxide; DREADDs, designer receptors exclusively activated by designer drugs; PVN, paraventricular nucleus of the hypothalamus; TAC, transascending aortic constriction.

FIGURE 3 Long-Term Activation of PVN Oxytocin Neurons Improves Heart Rate Recovery and Survival Rates in Animals With Heart Failure

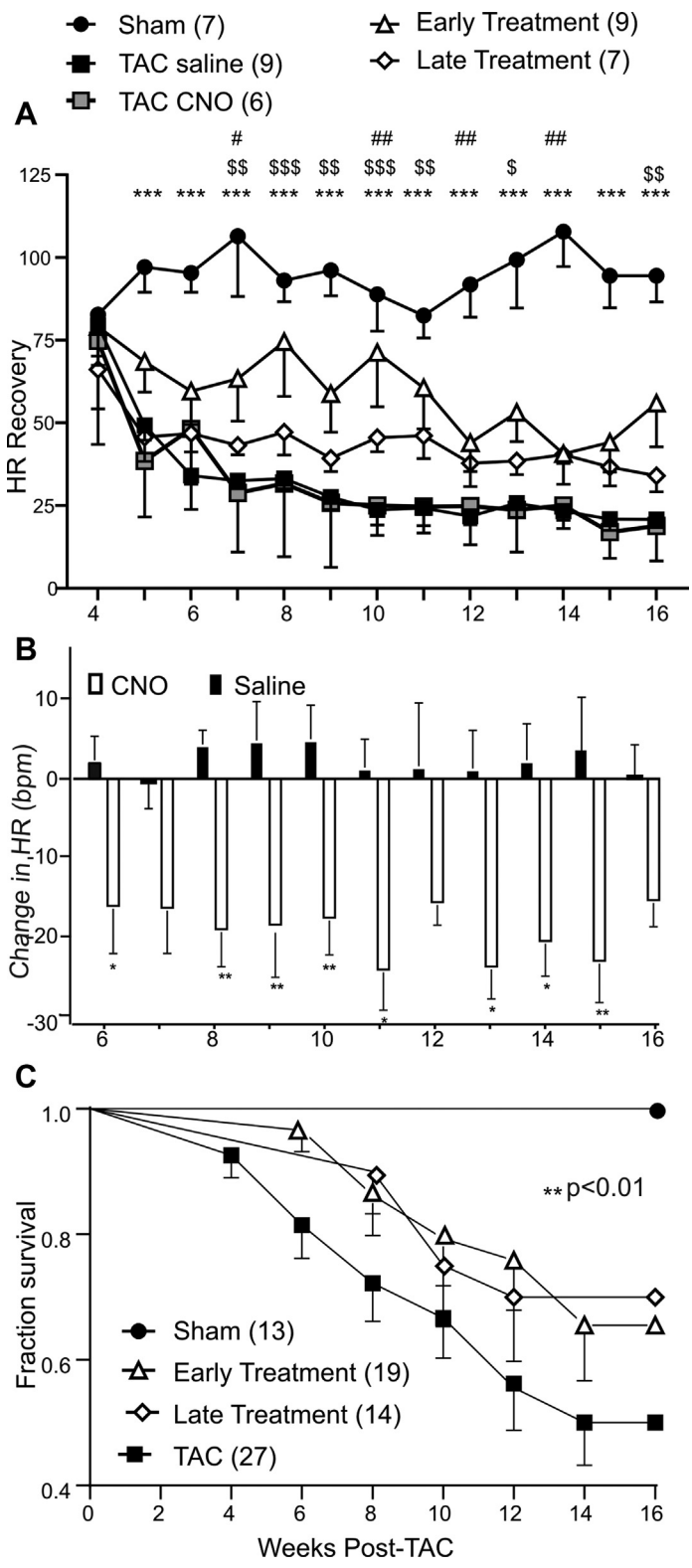

Continued on the next page

RESULTS

To test the hypothesis that synaptic release of OXT from hypothalamic OXT neurons at downstream autonomic targets is reduced in an animal model of HF, we quantified OXT release using engineered sniffer cells sensitive to OXT, in combination with photoactivation of ChR2 selectively expressed in PVN OXT neurons. Chinese hamster ovary (CHO) cells that expressed both OXT receptors and the red fluorescent genetically encoded Ca2+ indicator (R-GECO) were used as "sniffer cells," which are highly sensitive and selective biological sensors for the evoked photostimulated synaptic release of OXT (15). Selective expression of both ChR2 and an excitatory chemogenetic receptor for chronically activating PVN OXT neurons, DREADDs, was accomplished using 3 viral vectors in combination with the Cre-Lox system. Expression of the enzyme, Cre recombinase, was exclusively driven by the OXT promoter (rAAV1-OXT-Cre), stereotactically coinjected into the PVN of 1-week old pups with both floxed excitatory ChR2 (AAV1-EF1a-DIO-hChR2) and floxed excitatory DREADDs (AAV2-hSyn-DIO-hM3D(Gq), as previously described (12).

PVN synaptic terminals in the dorsal motor nucleus of the vagus (DMNX), a site of origin for preganglionic parasympathetic cardiac vagal neurons (CVNs), were identified, then surrounded by sniffer OXT-sensitive CHO cells, and photostimulated (Figure 1A). Photoactivation of ChR2 PVN OXT synaptic endings in the DMNX activated sniffer cells in Sham-operated animals with no significant changes in CHO cell responses at 2, 4, 6, 8, and 10 weeks postsurgery (Figure 1B and C). Pressure overload-induced HF was initiated in another group of animals using a TAC procedure to initiate progression to HF (11). In TAC animals, the photostimulated release of OXT, as detected by OXT-sensitive CHO cells, was significantly diminished at 6 and 10 weeks post-TAC (Figures 1B and 1C).

We next examined if chronic selective activation of PVN OXT neurons could restore OXT release in the DMNX following TAC. In this third group of animals, PVN OXT neurons were exclusively activated with chemogenetics via stimulation of excitatory DREADDs activated by daily intraperitoneal injections of CNO, 1 mg/kg/day, beginning at 4 weeks post-TAC, until animals were killed. In TAC + PVN OXT neuron-activated treatment animals, the release of OXT upon photoactivation of PVN synaptic terminals in the DMNX was similar to that of Sham animals at all time points, effectively attenuating TAC-induced diminished OXT release (Figures 1B and 1C).

In our previous work using this HF model, we have shown that there are no off-target effects of the DREADDs agonist CNO, or any biologically active metabolites, in nondisease (Sham) animals (16). In this study, we further tested for off-target effects of CNO or any biologically active metabolites by comparing 2 groups of TAC animals: a TAC group expressing DREADDS but receiving saline (TAC-saline) and a second TAC group, receiving CNO but not expressing DREADDs (TAC-CNO) (Figure 2). Treatment animals were divided into 2 groups: 1 with "early" PVN OXT neuron stimulation initiated at the onset of disease (4 weeks post-TAC) (Figure 2A) and the other with "late" treatment initiated at advanced progression of disease (6 weeks post-TAC). This was an important therapeutic time point because release

FIGURE 3 Continued

(A) Longitudinal weekly measurements of heart rate recovery at 20-s post-treadmill stress test in Sham, TAC saline (expressing DREADDs), TAC CNO (not expressing DREADDs), and early-, and late-treatment animals from 4 to 16 weeks post-Sham/TAC surgery. All groups of animals expressing DREADDs in PVN oxytocin neurons were implanted with DSI ETA-F10 telemetry devices at 2 weeks post-TAC to measure electrocardiography and heart rate. Excitatory DREADDs activation was achieved by intraperitoneal injections of CNO (1 mg/kg) starting at 4 weeks post-TAC in the early-treatment group and 6 weeks post-TAC in the late-treatment group until 16 weeks post-TAC; Sham and TAC saline animals received saline injections. Heart rate recovery (HRR) was calculated as the heart rate at peak exercise minus 20-s recovery postexercise. TAC animals displayed significantly lower HRR from 5 to 16 weeks post-TAC compared with Sham animals. Early treatment significantly improved HRR at 7 to 11 and 16 weeks post-TAC compared with TAC animals. Data were analyzed using mixed-effects model with Tukey's multiple comparison post-test. Sham ($n = 7$); TAC ($n = 9$); early treatment ($n = 9$); late treatment ($n = 7$); TAC CNO ($n = 6$). *Sham vs. TAC; $^{\$}$TAC vs. early treatment; *$p < 0.05$, **$p < 0.01$, ***$p < 0.001$. **(B)** Graph depicting changes in heart rate (beats per minute) in response to intraperitoneal injections of saline in TAC animals and CNO (1 mg/kg) in treatment animals from 6 to 16 weeks post-TAC/Sham. A significant reduction in heart rate was seen in all treatment animals at all weeks compared with saline-treated animals. Numbers in parentheses represent number of animals. Data were analyzed using mixed-effects model with Tukey's multiple comparison post-test; *$p < 0.05$. **(C)** Kaplan-Meier curves depicting percent survival in Sham, combined TAC saline (expressing DREADDs), and TAC CNO (not expressing DREADDs), early- and late-treatment animals. TAC animals had significantly reduced survival compared with Sham, whereas early and late treatment significantly improved survival rates in animals with heart failure. Data were analyzed using log-rank test of survival analysis; overall significance is represented as **$p < 0.01$. CNO = clozapine-N-oxide; DREADDs = designer receptors exclusively activated by designer drug; PVN = paraventricular nucleus of the hypothalamus; TAC = transascending aortic constriction.

FIGURE 4 Hearts From TAC Animals With PVN OXT Neuron Activation Had Improved LV Function and Less Collagen III and IL-1β Expression Compared with Untreated TAC Animals

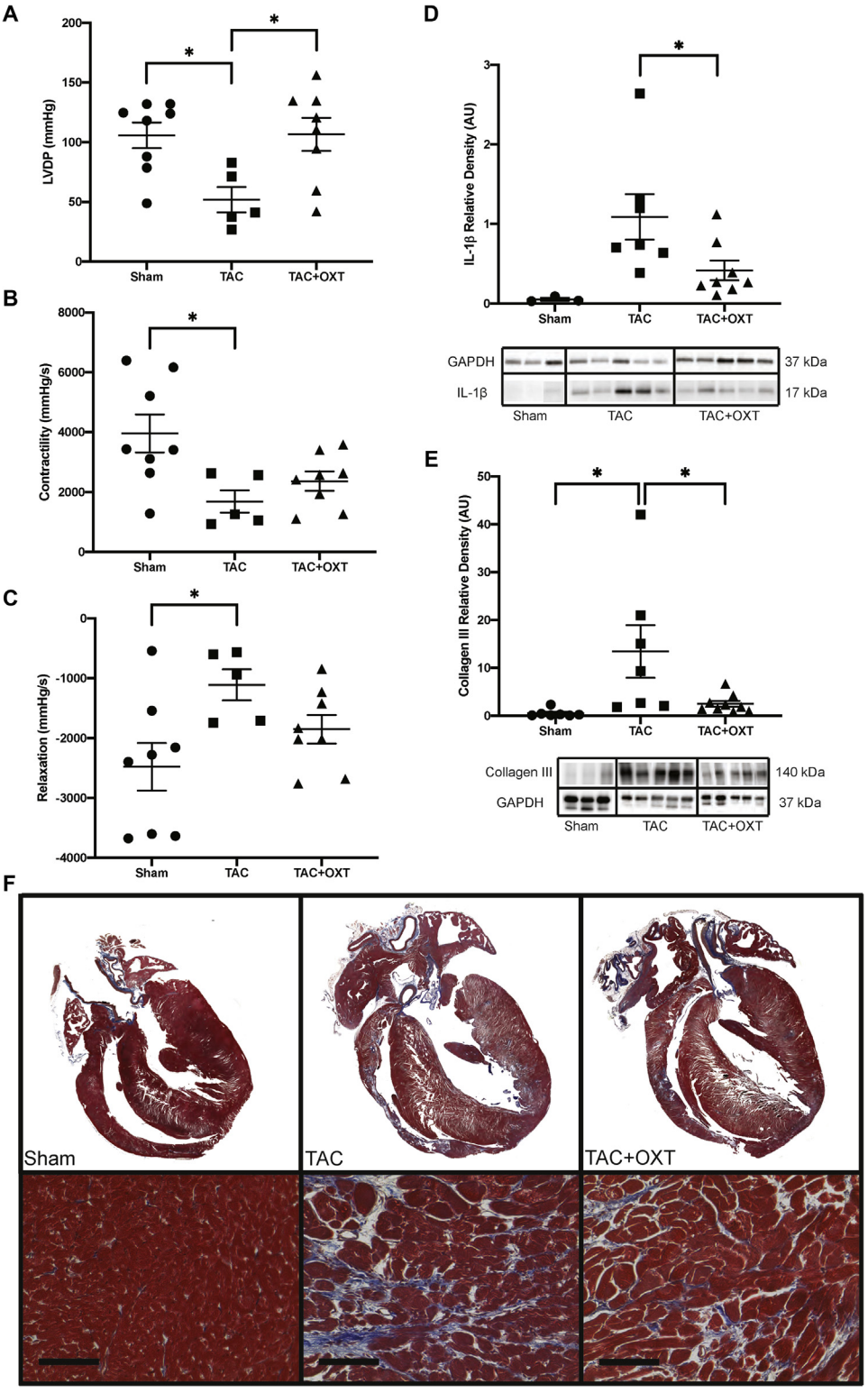

Continued on the next page

of OXT in the DMNX was lowest at 6 weeks post-TAC and cardiac dysfunction and mortality had been established (**Figures 2 and 3**). We examined longitudinal indices of cardiac function beginning at 2 weeks post-TAC, using high-resolution echocardiography (echo) in Sham, TAC (saline), TAC (CNO), and TAC + PVN OXT-activated animals. As expected, aortic velocity was 3-fold higher in each of the animal groups with TAC (TAC [saline], TAC [CNO], early and late treatments) compared with Sham animals (**Figure 2B**). Importantly, the degree of aortic narrowing, quantified by the increase in aortic velocity immediately downstream of the constriction, was not different in either of the TAC groups and treatment groups (**Figure 2B**). Indices of cardiac function—including stroke volume, EF, cardiac output, and FS—indicate preserved function with PVN OXT neuron treatment (early or late) compared with TAC (**Figures 2C to 2F**).

The benefit in cardiac function closely followed the timed initiation of PVN OXT neuron activation. In animals in which PVN oxytocin neurons were activated at 4 weeks, at the initial stage of disease initiation the benefit in cardiac function was observed beginning at the onset of treatment at 4 weeks post-TAC (**Figure 2**). Likewise, those animals that had late treatment (PVN OXT neuron-activated at 6 weeks post-TAC) when cardiac dysfunction was established, also showed benefits to cardiac function only beginning when treatment was started. From 8 to 16 weeks post-TAC, there were no significant differences in the improved cardiac function when comparing the 2 treatment groups, and both PVN OXT neuron-activated groups showed significant improvements in cardiac function compared with the untreated TAC group.

HRR after peak effort capacity is a common clinical assessment of autonomic balance and risk of adverse cardiovascular events, with a lower HRR associated with depressed parasympathetic activity and increased mortality (17). To assess HRR in each of the 5 groups of animals, ECG wireless transmitters were implanted 2 weeks post-TAC to measure the ECG and HR immediately following—and 20 s after—peak exercise treadmill tests (Naughton protocol). HRR values were lowest in TAC animals and significantly greater in animals in which PVN OXT neurons were activated both early (at 4 weeks post-TAC) and late (6 weeks post-TAC) compared with untreated TAC animals (**Figure 3A**). We then tested whether the change in HR responses to either daily CNO delivery or long-term activation of PVN OXT neurons were preserved throughout the treatment regimen. As shown in **Figure 3B**, the increase in parasympathetic activity to the heart, assessed as decreases in HR upon activation of PVN OXT neurons, shown previously to be blocked by muscarinic receptor blockade (16), persisted each week during the entire 16-week duration of this study. We next examined if PVN OXT neuron treatment reduced mortality following TAC-induced HF. There were no fatalities in the Sham group of animals during the course of the 16-week study (**Figure 3C**). The survival rate in TAC animals 16 weeks post-TAC was 50% and was significantly increased to 66% and 70%, respectively, in the early- and late-treatment animals (**Figure 3C**).

To elucidate potential intracardiac mechanisms responsible for the improvement in cardiac function following PVN OXT neuron activation, the expression of collagen III and the inflammatory marker, IL-1β, was measured by Western-blot analysis at the end of the study (16 weeks post-TAC). In addition, the isovolumic contractile function of hearts excised from animals was assessed during normal sinus rhythm. As cardiac function in both early- and late-treatment groups were not significantly different from each other at the end of the study, both treatment groups were combined for further analysis.

As expected, IL-1β expression was significantly higher in TAC animals compared with Sham-operated animals. PVN OXT treatment significantly attenuated

FIGURE 4 Continued

(A) Langendorff studies of excised hearts revealed that LVDP was significantly impaired in TAC animals (n = 5) compared with both Sham (n = 8) and PVN OXT treatment animals (n = 8). Contractility **(B)** and relaxation **(C)** measurements were calculated using the derivative of the LV pressure wave; both were significantly compromised in TAC animals (n = 5) compared with Sham animals (n = 8), whereas TAC + OXT animals (n = 8) did not significantly deviate from Sham. **(D)** Western-blot analysis revealed significant elevations in cardiac levels of IL-1β in TAC animals (n = 7) compared with PVN OXT treatment animals (n = 8) using a Student's *t*-test, as Sham levels were negligible; IL-1β quantitation is relative to GAPDH. **(E)** Western-blot assays also revealed significant elevations in cardiac levels of the fibrosis marker, collagen III, in TAC animals (n = 7) compared with both Sham (n = 7) and PVN OXT-treated animals (n = 9); collagen III quantitation is relative to GAPDH and to Sham values. **(F)** Trichrome-stained histological sections indicate increased fibrosis in all disease groups compared with Sham, as well as greater right-ventricular wall thinning in TAC-untreated animals compared with PVN OXT-treated animals. Data were analyzed using a 1-way analysis of variance with Tukey's *post hoc* test; *$p < 0.05$. GAPDH = glyceraldehyde-3-phosphate dehydrogenase; IL = inerleukin; LV = left ventricle; LVDP = left ventricle-developed pressure; PVN = paraventricular nucleus of the hyperthalamus; OXT = oxytocin; TAC = transascending aortic constriction.

FIGURE 5 Oxytocin Network That Increases Parasympathetic Activity to the Heart

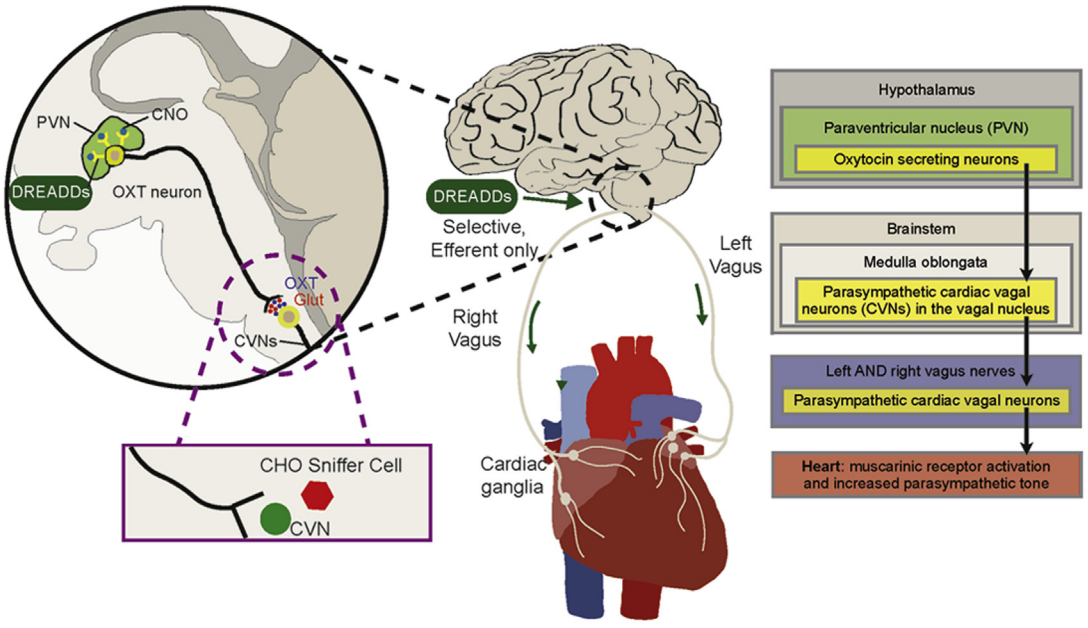

Selective channelrhodopsin-2 (ChR2) and excitatory designer receptors exclusively activated by designer drugs (DREADDs) expression in hypothalamic paraventricular nucleus (PVN) oxytocin (OXT) neurons was achieved with viral vectors that selectively expressed Cre under an OXT promoter and Cre-dependent vectors expressing either ChR2 or the excitatory hM3D(Gq) DREADDs. PVN OXT neuron activity was increased *in vivo* by daily injections of the DREADDs agonist, clozapine-N-oxide (CNO). Activation of PVN OXT neuron synaptic endings *in vitro* was accomplished by photoexcitation of ChR2. PVN OXT neurons corelease OXT and glutamate (Glut) to excite parasympathetic cardiac vagal neurons (CVNs) in the brainstem. The synaptic release of OXT was assessed using sniffer CHO cells that express both OXT receptors and the red fluorescent Ca2+ indicator (R-GECO) that were placed in close proximity to both PVN OXT synapses and their targeted CVNs. Increases in cardiac parasympathetic activity by activation of CVNs excites downstream parasympathetic cardiac ganglia neurons that release acetylcholine and activate muscarinic (M2) receptors in the heart.

this increase (**Figure 4D**, Supplemental Figure 1). Collagen III was likewise significantly higher in TAC animals than in Sham animals, and the expression of this fibrotic protein was significantly blunted in PVN OXT-treated animals (**Figure 4E**, Supplemental Figure 1). Trichrome histological sections suggest increased fibrosis in all disease groups compared with Sham; however right-ventricular wall thinning was more apparent in TAC animals compared with TAC treatment groups (**Figure 4F**). Cardiac function in excised hearts from these animals was examined using a Langendorff preparation in which the heart was perfused via the aorta at constant pressure (65 mm Hg). A size-5 balloon (Harvard Apparatus) was inserted into the LV to measure isovolumic LVDP. Contractility and relaxation were measured as the maximum and minimum values of the first derivative of the LVDP waveform, respectively, to assess inotropy and lusitropy, as we have previously described (16). TAC significantly impaired LVDP, and PVN OXT treatment attenuated this dysfunction (**Figure 4A**). Similarly, cardiac contractility and relaxation (**Figures 4B and 4C**) were significantly compromised in TAC compared with Sham animals; however, Sham- and PVN-treated animals did not vary significantly.

DISCUSSION

Parasympathetic activity to the heart originates in the brainstem and acts to reduce heart rate (18) and increase coronary flow (19,20). Our previous work has shown CVNs receive powerful excitation from a population of PVN OXT neurons that corelease OXT and glutamate to excite CVNs (12,15,21,22). Activation of excitatory DREADDs in PVN OXT neurons significantly reduces both blood pressure and HR in conscious unrestrained animals, and these decreases in blood pressure and HR are blocked by the muscarinic receptor antagonist atropine (16). The neuronal circuity and paradigm of this study, including the

activation of PVN OXT neurons with DREADDs in which OXT release is assessed by sniffer CHO cells surrounding CVNs—and the OXT network that increases parasympathetic activity to the heart—is shown in **Figure 5**. We have recently demonstrated that, in rats with LV hypertrophy that progresses to HF, CVNs have diminished excitation owing to both an increase in spontaneous inhibitory gamma aminobutyric acid (GABA)ergic neurotransmission frequency and a decrease in amplitude and frequency of excitatory glutamatergic neurotransmission to CVNs (11). Taken together, these findings suggested increasing excitatory input to CVNs—such as via the oxytocinergic PVN OXT/glutamate pathway—could be a promising approach to maintain cardiac parasympathetic activity, autonomic balance, and cardiac function during HF.

Using sniffer CHO cells as a novel approach to detect OXT, we have shown that photoactivated synaptic release of OXT from ChR2-expressing PVN fibers at brainstem targets (DMNX) where CVNs are localized is blunted in TAC animals but that this release can be restored with DREADDs-mediated selective activation of PVN OXT neurons. In **Figure 1**, we show that CHO cell responses were significantly blunted at 6 and 10 weeks but not 8 weeks post-TAC. Although we do not know the reason that the decrease at 8 weeks was not significantly different, it is likely due to the experimental design necessity of nonlongitudinal use of different groups of animals at each time point post-TAC. As PVN OXT release in the DMNX was lowest at 6 weeks post-TAC, we examined whether treatment by chronic PVN OXT neuron activation would benefit cardiac function, assessed both in vivo and ex vivo, as well as improve autonomic balance and reduce mortality. We began treatment in 1 group of animals early, at 4 weeks post-TAC, and another group late, at 6 weeks post-TAC, to reflect treatment further in progression of disease at a time when cardiac dysfunction has been established and mortality to the disease has begun.

Our results show that both early and late PVN OXT neuron activation improved mortality, as the survival rate in TAC animals—50%—was significantly improved to 66% and 70%, respectively, in the early- and late-treatment animals. PVN OXT neuron activation significantly mitigated the progression of cardiac dysfunction following TAC. Cardiac function indices, including EF, stroke volume, cardiac output, and FS all showed very similar improvements in animals with PVN OXT neuron activation, and those improvements followed a similar time course. Fibrosis, assessed by expression levels of collagen III, was significantly higher in TAC animals than in Sham animals, and this index of fibrosis was significantly blunted in PVN OXT-treated animals. Increased myocardial fibrosis is indicative of diffusive loss of working myocardium, which would increase wall stiffness while also having a negative impact on contractile function. Reduced ventricular compliance and increased perivascular collagen would also have a negative effect on vasodilatory reserve (23,24). Reduced coronary flow, plus the increased metabolic demands of pressure overload, would motivate ischemia, causing further myocardial damage. This would further increase fibrosis as myocytes were lost from ischemic injury, then replaced by collagen to maintain structural integrity (23), further reducing working myocardial mass. Indeed, in our *ex vivo* assessments of cardiac function, LVDP was significantly impaired in TAC animals and higher in treated animals. The LV hypertrophy observed in the untreated TAC animals was not reduced by PVN OXT neuron activation in the treated animals, but fibrosis and IL-1β levels were reduced, likely contributing to compensation mechanisms in the treatment groups that maintained a healthier myocardium.

HRR, an index of parasympathetic activity to the heart and a common clinical assessment of the risk of adverse cardiovascular events (with a lower HRR associated with increased mortality [17]), was lowest in TAC animals and significantly greater in early- and late-treatment animals. Consistent with these findings, HR responses to either daily CNO delivery or long-term activation of PVN OXT neurons were preserved throughout the treatment period as the decreases in HR upon activation of PVN OXT neurons was consistent upon testing each week throughout the entire 16-week duration of this study.

Beneficial outcomes observed with OXT neuron activation could be due to a number of downstream parasympathetic cardioprotective benefits. In addition to evidence that increasing parasympathetic activity to the heart decreases HR and increases coronary flow, PVN OXT neuron activation may have initiated a parasympathetic muscarinic receptor-mediated reduction in sympathetic activity. M2 muscarinic-receptor activation attenuates the production of cyclic adenosine monophosphate (AMP) to reduce the inotropic effects of β-adrenergic receptor activation in the ventricles (25,26). During long-term sympathetic stimulation, M2 activation reduces myocardial stress by lowering cyclic AMP to reduce the cellular hypercontractile state and increase relaxation during diastole, thereby improving myocyte viability (27) and slowing the progression of hypertrophy (28,29).

Although our work used an approach of selectively activating PVN OXT neurons, studies that have

JACC: BASIC TO TRANSLATIONAL SCIENCE VOL. 5, NO. 5, 2020
MAY 2020:484–97

activated downstream targets of PVN OXT neurons report similar increases in parasympathetic activity to the heart. Electrical stimulation of the parvocellular PVN evokes a bradycardia that is suppressed by application of an OXT receptor antagonist into the DMNX (30). In addition, a bradycardia is elicited upon injection of OXT into the DMNX, a response that is blocked by atropine (31). Basal HR varies inversely with dorsal brainstem oxytocin content, with the normal resting HR of normotensive rats associated with higher OXT content than in hypertensive animals (32), suggesting an important role of endogenous OXT release in the autonomic control of HR and the maintenance of a normal HR, autonomic balance, and blood pressure.

Overall, the improvements in cardiac function in HF we observed with PVN OXT neuron activation is consistent with the effects reported for other more invasive and poorly tolerated approaches to increase parasympathetic activity to the heart. Recent device-based approaches—such as implantable vagal stimulators that stimulate a multitude of visceral sensory and motor fibers in the vagus nerve (33) are being evaluated as new therapeutic approaches for HF (34,35). In animal studies, long-term vagal stimulation improves LV function, reduces infarct size, and decreases mortality (8). Despite initial promising clinical trials, a recent large-scale clinical study, NECTAR-HF (Neural Cardiac Therapy for Heart Failure), provided a negative result for chronic vagal nerve stimulation in patients with HF (36). There are many potential reasons for the lack of effect seen in this clinical study, which includes ineffective and/or nonspecific stimulation parameters (electrical stimulation amplitude and frequency) as well as the inherent disadvantage of activating noncardiac parasympathetic efferent fibers along with the sensory afferent fibers in the vagus nerve with vagal nerve stimulators (37). Our work in targeted activation of OXT neurons in the PVN provides an important step forward to determine if approaches that mimic PVN OXT neuron activation, such as noninvasive and well-tolerated intranasal administration of OXT, can increase parasympathetic activity to the heart in patients with HF, as it does in patients with obstructive sleep apnea (4), with, it is hoped, similar benefits of PVN OXT neuron activation shown in this animal model of HF.

ACKNOWLEDGMENT The authors thank Anastas Propitilloff (GWU Nanofabrication Center) for helping in acquiring confocal images.

ADDRESS FOR CORRESPONDENCE: Dr. David Mendelowitz, Department of Pharmacology and Physiology, George Washington University, 2300 Eye Street, NW,Washington, DC 20037. E-mail: dmendel@gwu.edu.

PERSPECTIVES

COMPETENCY IN MEDICAL KNOWLEDGE: Long-term restoration of the hypothalamic OXT network preserves OXT release, reduces mortality, cardiac inflammation, fibrosis, and improves autonomic tone and cardiac function in a model of heart failure.

TRANSLATIONAL OUTLOOK: This work provides the essential translational outlook to determine if approaches that mimic PVN OXT neuron activation, such as safe, noninvasive, and well-tolerated intranasal administration of OXT, can be beneficial in patients with HF.

REFERENCES

1. Althammer F, Grinevich V. Diversity of oxytocin neurones: beyond magno- and parvocellular cell types? J Neuroendocrinol 2018;30:e12549.

2. Gamer M, Büchel C. Oxytocin specifically enhances valence-dependent parasympathetic responses. Psychoneuroendocrinology 2012;37:87–93.

3. Norman GJ, Cacioppo JT, Morris JS, Malarkey WB, Berntson GG, Devries AC. Oxytocin increases autonomic cardiac control: moderation by loneliness. Biol Psychol 2011;86:174–80.

4. Jain V, Marbach J, Kimbro S, et al. Benefits of oxytocin administration in obstructive sleep apnea. Am J Physiol Lung Cell Mol Physiol 2017;313:L825–33.

5. Mozaffarian D, Benjamin EJ, Go AS, et al. Heart disease and stroke statistics: 2016 update, a report from the American Heart Association. Circulation 2016;133:e38–360.

6. Eckberg DL, Drabinsky M, Braunwald E. Defective cardiac parasympathetic control in patients with heart disease. N Engl J Med 1971;285:877–83.

7. Porter TR, Eckberg DL, Fritsch JM, et al. Autonomic pathophysiology in heart failure patients: sympathetic-cholinergic interrelations. J Clin Invest 1990;85:1362–71.

8. Klein HU, De Ferrari GM. Vagus nerve stimulation: a new approach to reduce heart failure. Cardiol J 2010;17:638–44.

9. Ishise H, Asanoi H, Ishizaka S, et al. Time course of sympathovagal imbalance and left ventricular dysfunction in conscious dogs with heart failure. J Appl Physiol 1998;84:1234–41.

10. Motte S, Mathieu M, Brimioulle S, et al. Respiratory-related heart rate variability in progressive experimental heart failure. Am J Physiol Heart Circ Physiol 2005;289:H1729–35.

11. Cauley E, Wang X, Dyavanapalli J, et al. Neurotransmission to parasympathetic cardiac vagal neurons in the brain stem is altered with left

ventricular hypertrophy-induced heart failure. Am J Physiol Heart Circ Physiol 2015;309:H1281–7.

12. Jameson H, Bateman R, Byrne P, et al. Oxytocin neuron activation prevents hypertension that occurs with chronic intermittent hypoxia/hypercapnia in rats. Am J Physiol Heart Circ Physiol 2016;310:H1549–57.

13. Jaimes R, Kuzmiak-Glancy S, Brooks DM, Swift LM, Posnack NG, Kay MW. Functional response of the isolated, perfused normoxic heart to pyruvate dehydrogenase activation by dichloroacetate and pyruvate. Pflügers Arch Eur J Physiol 2016;468:131–42.

14. Posnack NG, Brooks D, Chandra A, Jaimes R, Sarvazyan N, Kay MW. Physiological response of cardiac tissue to bisphenol A: alterations in ventricular pressure and contractility. Am J Physiol Heart Circ Physiol 2015;309:H267–75.

15. Piñol RA, Jameson H, Popratiloff A, Lee NH, Mendelowitz D. Visualization of oxytocin release that mediates paired pulse facilitation in hypothalamic pathways to brainstem autonomic neurons. PLoS One 2014;9:e112138.

16. Garrott K, Dyavanapalli J, Cauley E, et al. Chronic activation of hypothalamic oxytocin neurons improves cardiac function during left ventricular hypertrophy-induced heart failure. Cardiovasc Res 2017;113:1318–28.

17. Lachman S, Terbraak MS, Limpens J, et al. The prognostic value of heart rate recovery in patients with coronary artery disease: a systematic review and meta-analysis. Am Heart J 2018;199:163–9.

18. Grodner AS, Lahrtz H-G, Pool PE, Braunwald E. Neurotransmitter control of sinoatrial pacemaker frequency in isolated rat atria and in intact rabbits. Circ Res 1970;27:867–73.

19. Kovach JA, Gottdiener JS, Verrier RL. Vagal modulation of epicardial coronary artery size in dogs: a two-dimensional intravascular ultrasound study. Circulation 1995;92:2291–8.

20. Van Winkle DM, Feigl EO. Acetylcholine causes coronary vasodilation in dogs and baboons. Circ Res 1989;65:1580–93.

21. Dyavanapalli J, Dergacheva O, Wang X, Mendelowitz D. Parasympathetic vagal control of cardiac function. Curr Hypertens Rep 2016;18:22.

22. Piñol RA, Bateman R, Mendelowitz D. Optogenetic approaches to characterize the long-range synaptic pathways from the hypothalamus to brain stem autonomic nuclei. J Neurosci Methods 2012;210:238–46.

23. Weber KT, Sun Y, Guarda E. Structural remodeling in hypertensive heart disease and the role of hormones. Hypertension 1994;23:869–77.

24. Strauer BE. Development of cardiac failure by coronary small vessel disease in hypertensive heart disease? J Hypertens Suppl 1991;9:S11–20; discussion S20–1.

25. Bers DM. Cardiac excitation-contraction coupling. Nature 2002;415:198–205.

26. Bristow MR, Ginsburg R, Umans V, et al. Beta 1- and beta 2-adrenergic-receptor subpopulations in nonfailing and failing human ventricular myocardium: coupling of both receptor subtypes to muscle contraction and selective beta 1-receptor down-regulation in heart failure. Circ Res 1986;59:297–309.

27. Pepper GS, Lee RW. Sympathetic activation in heart failure and its treatment with beta-blockade. Arch Intern Med 1999;159:225–34.

28. Harvey RD, Belevych AE. Muscarinic regulation of cardiac ion channels. Br J Pharmacol 2003;139:1074–84.

29. Henning RJ, Sawmiller DR. Vasoactive intestinal peptide: cardiovascular effects. Cardiovasc Res 2001;49:27–37.

30. Rogers RC, Hermann GE. Hypothalamic paraventricular nucleus stimulation-induced gastric acid secretion and bradycardia suppressed by oxytocin antagonist. Peptides 1986;7:695–700.

31. Rogers RC, Hermann GE. Dorsal medullary oxytocin, vasopressin, oxytocin antagonist, and TRH effects on gastric acid secretion and heart rate. Peptides 1985;6:1143–8.

32. Michelini LC. Differential effects of vasopressinergic and oxytocinergic pre-autonomic neurons on circulatory control: reflex mechanisms and changes during exercise. Clin Exp Pharmacol Physiol 2007;34:369–76.

33. Yamakawa K, So EL, Rajendran PS, et al. Electrophysiological effects of right and left vagal nerve stimulation on the ventricular myocardium. Am J Physiol Circ Physiol 2014;307:H722–31.

34. Schwartz PJ, De Ferrari GM, Sanzo A, et al. Long term vagal stimulation in patients with advanced heart failure First experience in man. Eur J Heart Fail 2008;10:884–91.

35. Buckley U, Shivkumar K, Ardell JL. Autonomic regulation therapy in heart failure. Curr Heart Fail Rep 2015;12:284–93.

36. De Ferrari GM, Tuinenburg AE, Ruble S, et al. Rationale and study design of the NEuroCardiac TherApy foR Heart Failure Study: NECTAR-HF. Eur J Heart Fail 2014;16:692–9.

37. Bendary A, Bendary M, Salem M. Autonomic regulation device therapy in heart failure with reduced ejection fraction: a systematic review and meta-analysis of randomized controlled trials. Heart Fail Rev 2019;24:245–54.

KEY WORDS heart failure, oxytocin, parasympathetic

APPENDIX For a supplemental figure, please see the online version of this paper.